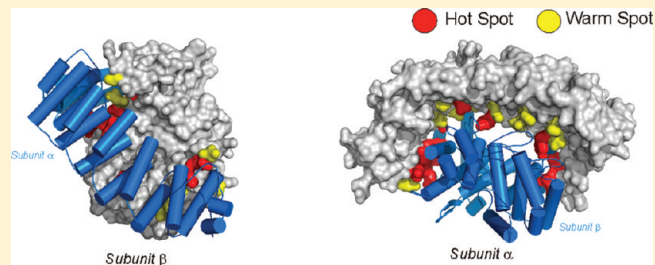


Detection of Farnesyltransferase Interface Hot Spots through Computational Alanine Scanning Mutagenesis

Marta A. S. Perez, Sérgio F. Sousa, Eduardo F. T. Oliveira, Pedro A. Fernandes, and Maria J. Ramos*

REQUIMTE, Departamento de Química e Bioquímica, Faculdade de Ciências, Universidade do Porto, Rua do Campo Alegre, 687, 4169-007 Porto, Portugal

ABSTRACT: In this study, we present a detailed characterization of the full α/β interface in the farnesyltransferase (FTase) enzyme, an important target in drug design efforts. This characterization is presented in terms of hot spots, warm spots, and null spots and is based on the application of an improved variation of the computational alanine scanning mutagenesis methodology, complemented with extensive solvent-accessible surface area and interfacial hydrogen-bonding analysis. A total of 130 interface amino acid residues were considered in this analysis, a number that represents 16.0% of the total of 814 amino acid residues in the full enzyme. Globally, the results provide important clues on the most important structural and energetic determinants for dimer formation, suggesting several key targets at the subunit interface for the development of new molecules that aim to inhibit FTase activity through blocking the formation of the fully active FTase dimer, yielding useful indications for future drug design efforts.



INTRODUCTION

The enzyme farnesyltransferase (FTase) has been for the past 15 years at the center of intense research in the development of a new class of anticancer drugs: the farnesyltransferase inhibitors (FTIs).^{1–4} Interest in this enzyme and this new class of anti-cancer drugs was initially prompted by the discovery that farnesylation was absolutely required for the oncogenic forms of Ras proteins to transform cells.^{5–7} This finding was of particular importance since mutant Ras proteins were known to be implicated in something like 30% of all human cancers.^{8–10} In the years that followed, more than 400 patents describing FTIs were reported, with several of these compounds moving into clinical trials for cancer treatment.^{2,11–20} The outcome of the clinical trials was, however, far less exciting than the one envisioned from the preclinical studies, with the most advanced FTIs failing to demonstrate antitumor activity in ras-dependent cancers.^{21,22} In fact, K-ras, the major most frequently mutated form of ras in human cancers, is able to bypass FTI blockade through cross-prenylation by the related geranylgeranyltransferase I.^{23–25} More recently, however, the application of FTIs began to be explored in other types of cancers (non-ras-dependent), most notably on breast cancer,^{26–31} and on hematological malignancies, including chronic myeloid leukemia, advanced myelodysplastic syndrome, chronic myelomonocytic leukemia, acute lymphoblastic leukemia, acute myeloid leukemia, and multiple myeloma.^{32–38} Accounting for the observed antitumor activity of such farnesyltransferase inhibitors remains an unanswered question, with a number of possible targets discussed in literature whose inhibition may contribute to this effect. RhoB;^{39–42} the centromere binding proteins CENP-E and CENP-F;^{43–45} the phosphatase PRL1, 2, and 3;^{46,47} RheB (ras homologue enriched in brain);⁴⁸ and the

nuclear lamins⁴⁹ are just a few examples. Possible roles in the treatment of some parasitic infections—in particular, malaria^{50–55} and the African sleeping sickness^{56–58}—have been explored, too. Other more recently suggested applications of FTIs include the treatment of progeria^{59–62} and of tuberous sclerosis.¹⁸

FTase is a heterodimeric zinc metalloenzyme composed of two subunits (α and β) that catalyzes the farnesylation of protein substrates containing a C-terminal CAAX motif, in which C is the cysteine that is farnesylated; “A” is usually an aliphatic amino acid; and X is the terminal amino acid, normally methionine, serine, alanine, or glutamine.^{63–67} Farnesylidiphosphate (FPP) is the typical isoprenoid farnesyl donor, and the Ras family of proteins, nuclear lamins A and B, and the γ subunit of heterotrimeric G-proteins are among the known CAAX substrates for FTase.^{68–70}

The high strategic interest attributed to FTase in pharmacologic research efforts has resulted in a vast set of studies focusing on the specific characteristics of this enzyme in terms of structure and activity, with the first X-ray crystallographic structure for this enzyme being published in 1997.⁷¹ Today, more than 50 X-ray crystallographic structures have been published, including structures with different catalytic intermediate states, with different substrates and inhibitors, and with different mutations. A large number of kinetics, mutagenesis, and EXAFS studies have also been made available,^{72–81} contributing to a better understanding of FTase activity, even though several doubts arising from the existence of apparently contradicting experimental evidence have persisted.⁸²

Received: June 11, 2011

Revised: November 7, 2011

Published: November 07, 2011

Computational studies by our research group^{83–87} and by several other research groups^{88–90} were then employed to rationalize and reconcile the existing mechanistic doubts, providing a detailed atomistic picture of the activity of this enzyme, a process that culminated with the finding and characterization of the elusive transition state structure for the critical farnesylation step.^{91,92}

In the context of this quest and following our work on establishing a well-grounded computational/experimental unified view on Zn coordination spheres formed at the several intermediate states on the catalytic mechanism of this enzyme,^{83,84,86} a set of specific force field parameters able to accurately describe the several metal coordination spheres formed along the catalytic pathway of this enzyme and committed to the AMBER force field have been derived and extensively validated,⁹³ opening the door to future studies on the full enzyme through molecular dynamics (MD) simulations or MD-based methodologies.

Alanine scanning mutagenesis (ASM) is a very powerful tool for the study of protein–protein or subunit interfaces⁹⁴ that can be applied to identify the amino acid residues that are responsible for most of the binding energy between the two components that make up the interface. The most important residues at these regions are called hot spots and have been defined as those residues that upon alanine mutation result in a binding free energy difference of 4.0 kcal/mol or greater.^{95,96} Other relevant residues for the binding process between subunits are the warm spots, which upon alanine mutation result in a binding free energy difference of between 2.0 and 4.0 kcal/mol. Amino acid residues that upon alanine mutation result in a binding free energy difference of between 2.0 and 0.0 kcal/mol are called null-spots and below this 0.0 kcal/mol threshold are called cold-spots.^{95,96}

Over time, several studies have taken advantage of this methodology to scan protein–protein interfaces and subunit–interfaces in search of the most important regions for interaction. This basic idea behind most of this research is that the knowledge of these regions not only could allow a better understanding of protein–protein association and the activity of such systems but also could serve as a basis for the development of new inhibitors designed to bind the most determinant residues at the interface as a strategy to hinder the formation of the resulting complexes, thereby blocking the activity of the protein–protein complex. Some systematic ASM studies have indicated that hot spots tend to be particularly enriched in tryptophan (21%), tyrosine (12%), and arginine (13%).^{97,98} Interestingly, some studies have suggested that the hot spots are usually surrounded by residues not important for binding whose role would be to shelter the hot spots from the solvent.⁹⁷ Such structures resembled an O-ring, a likeness that resulted in the name given to this proposal: the O-ring hypothesis.

Despite the valuable insight that ASM methodologies could offer in the study of protein–protein interfaces, experimental alanine scanning mutagenesis is a slow, labor-intensive, and expensive methodology. These limitations are particularly relevant when the interface between different proteins subunits in a protein or between different proteins in a protein–protein complex is very large, as it is the case of the enzyme FTase. This enzyme is composed of a 48 kDa α -subunit consisting of 379 amino acid residues, and a second 46 kDa β -subunit with 437 amino acid residues, arranged to give a global protein with a subunit interface defined by 130 amino acid residues (59 from the α -subunit; 71 from the β -subunit), which buries $\sim 3300 \text{ \AA}^2$ of solvent-accessible surface area.⁷¹

Computational alanine scanning mutagenesis was developed as an alternative to the experimental ASM, allowing such large interfaces to be efficiently analyzed for the presence of hot spots, warm spots, and null spots. Several different formulations, mainly based on the application of MD simulations or the use of knowledge-based scoring functions, have been described in the literature, at different levels of sophistication and computational cost, and with different levels of success.^{99–106} In particular, a variation of the standard computational ASM method (based on MD)¹⁰⁴ has been developed at our group.¹⁰⁷ It is based on the use of the well-established but slower MM-PBSA (molecular mechanics/Poisson–Boltzmann surface area) approach,¹⁰⁴ optimized for the use of a continuum solvation description considering different internal dielectric constant values for different types of amino acid residues, and has been shown to yield particularly highly accurate results in a variety of different biological systems,^{108–110} with an overall success rate of 80% in the identification of hot spots and warm spots.¹⁰⁷

In this study, we have applied the computational alanine scanning mutagenesis method developed at our research group,¹⁰⁷ together with the set of molecular mechanical parameters also in-house specifically tailored to describe the Zn coordination sphere in FTase,⁹³ to quantitatively characterize each residue of the α/β interface in terms of the relative binding free energy between the wild type and the mutant. These results allowed us to describe the full FTase α/β interface in terms of hot spots, warm spots, null spots, and cold spots and to subdivide the interface region into different contributions. The knowledge arising from this analysis provides important clues about the association determinants for the two FTase subunits and could serve as a basis for the development of a new class of FTIs, designed to block the association of the two subunits to yield the fully active FTase heterodimeric form.

METHODS

Model Setup and Molecular Dynamics Simulations. The initial model was prepared from the only X-ray crystallographic structure available on the RCSB Protein Data Bank¹¹¹ of FTase in the absence of any substrate or inhibitor: structure 1FT1 (resolution 2.25 Å).⁷¹ This structure contains 315 residues from the α -subunit (residues 55–369) and 415 residues from the β -subunit (residues 23–437). Conventional protonation states for all amino acids at pH 7 were considered. All the hydrogen atoms were added using the LEAP program in the AMBER 9.0 Software package.¹¹² The dimension of the system was 11 498 atoms.

A set of molecular mechanics parameters specifically designed and optimized to describe the Zn coordination sphere in the FTase resting state⁹³ and based on DFT and molecular mechanical calculations,^{83–87} crystallographic data,^{71,113,114} extended X-ray absorption fine structure (EXAFS) results,⁷⁹ and on several other mechanistic studies^{77,78,115,116} was considered. The parameters describe the Zn metal coordination sphere at the resting state as being distorted tetracoordinated with the metal covalently bound to the amino acid residues Asp297 β (bidentate coordination), Cys299 β , and His362 β , following the bonded-model approach introduced by Hoops et al.¹¹⁷ The parameters used are described in detail elsewhere, together with the parametrization and validation methods, and with the premises adopted⁹³ and have already been used with success in the study of FTase through MD simulations.^{118–120} Standard amino acid

residues were accounted for by the use of the Cornell et al. AMBER force field.¹²¹

The effect of the solvent was described through the use of the Hawkins, Cramer, Truhlar pairwise generalized Born model,^{122,123} with the parameters described by Tsui and Case,¹²⁴ as implemented in AMBER 9.0.

The system was subjected to a three-stage refinement protocol using the SANDER module of AMBER 9.0 in which the constraints on the enzyme were gradually removed. In the first stage (10 000 steps), 50 kcal/mol/Å² harmonic forces were used to restrain all the heavy atoms in the system, allowing the hydrogen atoms added with LEAP to adjust. In a second stage (30 000 steps), these constraints were limited to the CA and N atom-type atoms (backbone α -carbons and nitrogens). Finally, a full energy minimization (third stage, maximum 80 000 steps) was performed until the rms gradient was smaller than 0.0002 kcal mol⁻¹ Å⁻¹.

Subsequently, a 10 ns MD simulation was performed starting from the minimized structure. Bond lengths involving hydrogens were constrained using the SHAKE algorithm,¹²⁵ and the equations of motion were integrated with a 2 fs time-step being. A nonbonded interaction cutoff radius of 16 Å, and the Langevin thermostat was used to maintain the temperature of the system at 310 K.

Computational Alanine Scanning Mutagenesis. Our alanine scanning mutagenesis methodology uses a single MD trajectory of the wild type system to calculate the binding free energies. From this trajectory, each interfacial residue of the FTase subunits is mutated to alanine, allowing the differences in the binding free energy ($\Delta\Delta G_{\text{binding}}$) for each mutation in relation to the wild type to be calculated with the MM-PBSA approach, optimized by considering different internal dielectric constant values for different types of amino acid residues.

The use of a single trajectory in this process to calculate $\Delta\Delta G_{\text{binding}}$ has been shown to give a better agreement with the experimental data than the use of multiple trajectories.¹⁰⁷ In fact, for the use of a single trajectory, error cancellation has been assumed to overcome the inaccuracies due to the reduced sampling of the conformational space in MD simulations at the nanosecond time scale.^{126,127}

Following these general principles, the MM-PBSA script implemented in AMBER was used to perform a postprocessing treatment of the FTase α/β dimer by using the structure of the full enzyme and calculating its respective energy and those of the interacting monomers (α and β). To generate the structure of the alanine mutants, a simple truncation of the mutated side chain was made, replacing C_γ with a hydrogen atom and setting the alanine C_β —H bond direction to that of the former C_γ — C_β . For the binding free energy calculations, 60 snapshots were extracted from the last 6000 ps of the MD run (one at every 100 ps interval).

The calculation of the entropic contribution is computationally expensive because it requires extremely well minimized structures for a normal-mode analysis or large numbers of snapshots for a quasi-harmonic analysis.^{127–129} For this reason, in the calculation of relative free energy differences between two sets of structures of related complexes, it is normally assumed that the entropic contribution to the absolute free energies cancel out.^{107,130–132} In the particular case of the computational ASM methods that are based on the postprocessing treatment of a single MD simulation run on the native complex, such as the one applied in this work, the snapshots considered in the analysis will be virtually identical in the native and mutant structures. In such

cases, the only difference will be in the side chain that is mutated, which in the case of FTase will be one amino acid from a total of \sim 800 amino acid residues. Hence, it is expected that the entropy contribution would also be close to identical for native and mutant structures. Previous computational ASM base studies under less favorable conditions have estimated \sim 0.25 kcal/mol for this contribution.¹³³ In this work, we have calculated the difference in the entropic contribution by normal-mode analysis for the Tyr200 α mutation to alanine considering 60 snapshots, obtaining an entropic difference of 0.31 kcal/mol. This contribution is expected to be even smaller for smaller amino acid residues, particularly for those that exhibit a very small accessible surface area, such as most of the ones included in this study, which focus on the FTase interface.

The ASM protocol used here, developed in our research group and based on the well-known MM-PBSA approach,^{104,130,134} has been used with success in the study of several biological systems, including the IgG1 streptococcal protein G (C2 fragment) complex,¹⁰⁸ the ZipA:FtsZ complex, the complex formed between hen egg white lysozyme (HEL) and the antibody HyHEL-10,¹⁰⁹ the MDM2-P53 complex,¹¹⁰ and HIV-1 protease,¹³² and in previous benchmarking studies against experimental data has been shown to have an overall success rate of 80% in identifying hot spots and warm spots and to yield a mean unsigned error of around 0.8 kcal/mol.

SASA Analysis. Solvent-accessible surface area values were calculated for all interface amino acid residues using the program Visual Molecular Dynamics¹³⁵ and considering the standard probe radius for water of 1.4 Å. From the MD simulations performed and for each residue, SASA values were calculated, for a total of 3000 MD snapshots from the last 6 ns of simulation, considering (1) the full dimer, SASA_{dimer}; (2) only the residues from the same subunit of each amino acid residue evaluated, neglecting the shielding effect of the other subunit, SASA_{monomer}, and yielding a value for the potential SASA of that specific residue in the monomer. Final values are expressed as a percentage of the potential SASA for the free residue, a quantity that was estimated from the MD trajectory for each residue, while neglecting the solvent shielding effect of all the other amino acid residues from both subunits into each specific amino acid.

Mutant Selection. Residues to mutate were selected from a detailed analysis of the FTase α/β interface in the 1FT1 interface, based on the PDBsum database.^{136,137} This database provides an at-a-glance overview of every macromolecular structure deposited in the Protein Data Bank, giving schematic diagrams of the molecules in each structure and of the interactions between them.

A total of 130 interface residues were identified. From these, a total of 111 mutations were effectively evaluated using the ASM protocol outlined above (53 in the α -subunit and 58 in the β -subunit), yielding $\Delta\Delta G_{\text{binding}}$ values in relation to the wild-type enzyme.

Alanine scanning mutagenesis of alanine residues is a redundant process. Glycine has a smaller side chain than alanine and, hence, cannot be effectively mutated to alanine in a consistent fashion within the protocol considered for the other amino acids. In fact, in glycine, the absence of a side chain confers to the backbone an additional conformational freedom that typically results in relevant structural rearrangements at the backbone. Hence, the experimental measure of the $\Delta\Delta G_{\text{binding}}$ for such mutation does not correspond to the subunit interaction difference between glycine and alanine but, rather, to a more global interaction difference that also includes the backbone rearrangement

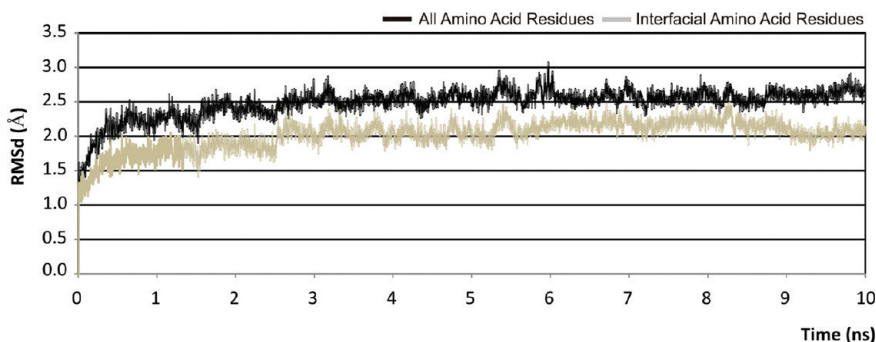


Figure 1. RMSd analysis of the backbone atoms in the MD simulations of FTase. Particular attention is dedicated to the behavior of the interface amino acid residues.

Table 1. Average Differences in Binding Free Energies ($\Delta\Delta G_{\text{Binding}}$) between the Wild Type FTase and the Alanine Mutant Variants and Average Solvent Accessible Surface Areas (SASA) for the Hot Spots, Warm Spots, And Null Spots Identified and Corresponding Standard Deviation^a

Type	Subunit	Number of Residues	$\Delta\Delta G_{\text{Binding}}$ (kcal/mol)	SASA lost upon Dimerization		
				Average SASA _{Monomer} (%)	Average SASA _{Dimer} (%)	(%)
Hot Spots	Monomer α	13	8.11 (0.26)	39.9 (7.7)	3.5 (2.0)	36.4 (7.8) 105.9 (22.8)
	Monomer β	11	6.57 (0.25)	29.8 (15.5)	3.5 (3.4)	26.3 (13.1) 78.9 (41.0)
	Total	24	7.40 (0.26)	35.3 (11.6)	3.5 (2.7)	31.8 (10.4) 93.5 (31.9)
Warm Spots	Monomer α	14	2.93 (0.20)	26.5 (12.0)	7.6 (5.6)	18.9 (9.5) 54.8 (30.6)
	Monomer β	11	2.63 (0.27)	33.9 (11.7)	12.7 (8.6)	21.2 (8.7) 59.7 (27.4)
	Total	25	2.80 (0.24)	29.8 (11.8)	9.9 (7.1)	19.9 (9.1) 57.0 (29.0)
Null Spots	Monomer α	19	0.82 (0.20)	30.5 (11.0)	18.3 (10.8)	12.2 (4.3) 33.2 (11.1)
	Monomer β	17	1.06 (0.25)	25.0 (10.4)	10.4 (7.8)	14.6 (5.5) 42.9 (16.5)
	Total	36	0.93 (0.25)	27.9 (10.7)	14.6 (9.3)	13.4 (4.9) 37.8 (13.8)
Cold Spots	Monomer α	7	-1.26 (0.30)	23.8 (16.0)	11.9 (11.1)	11.9 (8.7) 35.1 (28.2)
	Monomer β	19	-1.58 (0.20)	21.1 (11.8)	11.6 (6.4)	9.5 (10.3) 25.4 (31.0)
	Total	26	-1.50 (0.26)	21.8 (14.4)	11.7 (8.3)	10.2 (9.5) 28.0 (29.6)

^a Hot spots, grey and bold; warm spots, bold.

effects. This is an obvious limitation of the experimental ASM method that could be eventually surpassed computationally; namely, with the use of a single trajectory. The difficulty here lies in the lack of experimental reference values for glycine–alanine mutations, essential to fully calibrate the computational ASM method employed to treat all the other amino acid residues in this study.

A similar problem can be highlighted for proline. In fact, the proline ring restricts the geometry of the backbone chain in the proteins where it is present, sometimes resulting in a backbone conformation very different from the one adopted when an alanine or any other residue is present. Experimental ASM of proline is therefore particularly troublesome, as it can produce abnormal changes to the binding free energies as a result of the backbone conformational differences, masking the results.^{98,107} For these reasons, proline residues were also not evaluated.

Calculation of Conservation Grades. The ConSurf-HSSP database¹³⁸ was used to obtain estimated conservation grades for

each amino acid position along the FTase sequence. This database contains conservation scores calculated by the Rate4-Site algorithm¹³⁹ for each amino acid position within each three-dimensional protein structure present in the related Homology-derived Secondary Structure of Proteins (HSSP) database,^{140,141} which holds multiple sequence alignments for three-dimensional protein structures from the Protein Data Bank. A total of 28 amino acid sequences were considered for the α -subunit, whereas for the β -subunit, the total number was 78 sequences. The ConSurf-HSSP database may be accessed at <http://consurf-hssp.tau.ac.il> or via the PDbsum Web site, <http://www.ebi.ac.uk/thornton-srv/databases/pdbsum/>.

RESULTS AND DISCUSSION

1. General Analysis of the MD Simulations. Figure 1 illustrates the root-mean-square deviation (RMSd) values for

Table 2. Differences in the Binding Free Energies ($\Delta\Delta G_{\text{Binding}}$) and Standard Deviation for the Wild Type FTase and Alanine Mutant Variants Calculated^{a,b}

Interfacial Analysis - Monomer α					
Residue	$\Delta\Delta G_{\text{Binding}}$ (kcal/mol)	SASA _{Monomer} (%)	SASA _{Dimer} (%)	SASA _{Lost} (%)	SASA _{Lost} (Å ²)
Gln80	0.44 (0.75)	38.3 (1.9)	24.9 (1.6)	13.5 (2.5)	38.5 (7.3)
Asn81	0.95 (0.82)	36.0 (1.2)	16.6 (1.6)	19.4 (2.0)	49.6 (5.0)
Asp82	-1.79 (0.64)	55.4 (1.1)	46.9 (1.5)	8.5 (1.8)	21.2 (4.5)
Ser85	0.47 (0.75)	40.0 (0.8)	22.0 (1.0)	17.9 (1.3)	39.6 (2.9)
Val87	6.70 (1.29)	48.0 (0.8)	0.9 (0.3)	47.1 (0.8)	118.5 (2.1)
Val88	8.19 (1.26)	51.9 (0.4)	0.9 (0.2)	50.9 (0.4)	130.7 (1.1)
Gln89	1.04 (0.73)	29.1 (1.3)	12.9 (1.1)	16.2 (1.7)	46.0 (4.8)
Ile90	6.41 (1.28)	38.7 (0.7)	1.4 (0.4)	37.3 (0.8)	104.3 (2.2)
Ile91	0.88 (1.27)	59.6 (0.7)	38.6 (0.8)	21.0 (1.1)	57.9 (3.1)
Tyr92	-1.39 (0.81)	23.9 (1.0)	15.8 (1.1)	8.1 (1.4)	26.3 (4.7)
Ser93	1.78 (0.74)	31.4 (0.7)	23.1 (0.6)	8.3 (0.9)	18.5 (2.1)
Phe96	0.15 (1.26)	14.1 (0.6)	2.5 (0.4)	11.6 (0.7)	36.1 (2.1)
Leu107	0.04 (1.27)	19.6 (0.5)	4.0 (0.5)	15.6 (0.7)	44.2 (2.1)
Asn127	0.67 (0.84)	20.6 (0.8)	4.1 (0.5)	16.4 (0.9)	42.4 (2.4)
Tyr131	6.21 (0.84)	42.1 (0.8)	4.7 (0.5)	37.4 (0.9)	121.3 (3.0)
Thr132	2.80 (0.85)	13.8 (0.4)	0.2 (0.2)	13.6 (0.5)	32.9 (1.2)
His135	3.34 (0.74)	33.5 (0.6)	4.7 (0.6)	28.8 (0.9)	82.2 (2.5)
Tyr166	2.31 (0.82)	45.2 (1.4)	21.7 (1.7)	23.4 (2.2)	76.9 (7.2)
His170	2.49 (0.73)	24.9 (0.5)	9.0 (0.5)	15.8 (0.7)	45.3 (2.0)
Arg173	1.78 (0.63)	17.5 (0.8)	10.1 (0.6)	7.4 (1.0)	25.6 (3.5)
Lys198	-2.12 (0.62)	48.0 (0.8)	5.7 (0.6)	42.4 (1.1)	134.0 (3.4)
Tyr200	8.17 (0.83)	50.8 (0.7)	7.9 (0.5)	42.9 (0.8)	136.8 (2.7)
Gln204	3.65 (0.73)	7.5 (0.5)	2.8 (0.7)	4.8 (0.9)	13.7 (2.5)
Gln207	0.68 (0.74)	17.0 (0.5)	3.6 (0.5)	13.4 (0.7)	39.2 (2.0)
Asp230	3.42 (0.63)	24.6 (0.4)	8.4 (0.4)	16.3 (0.6)	39.5 (1.4)
Arg232	3.53 (0.65)	45.0 (0.7)	3.2 (0.4)	41.8 (0.8)	146.5 (2.8)
Asn234	3.93 (0.81)	38.4 (0.4)	0.9 (0.3)	37.6 (0.5)	95.9 (1.3)
Ser235	3.24 (0.76)	10.9 (0.3)	0.8 (0.2)	10.1 (0.3)	22.7 (0.7)
Asn238	15.61 (0.83)	33.3 (0.4)	1.7 (0.2)	31.6 (0.5)	81.1 (1.2)
His241	2.07 (0.74)	21.4 (0.6)	12.1 (0.6)	9.3 (0.8)	26.7 (2.4)
Leu269	1.07 (1.25)	45.3 (0.6)	35.5 (1.1)	9.8 (1.3)	27.9 (3.6)
Val270	-2.86 (1.23)	12.9 (0.5)	2.1 (0.4)	10.8 (0.6)	27.4 (1.5)
His272	3.78 (0.75)	34.8 (0.6)	9.1 (0.5)	25.8 (0.8)	74.3 (2.3)
Asn273	2.00 (0.82)	1.2 (0.2)	0.4 (0.2)	0.8 (0.3)	2.1 (0.8)
Glu274	9.44 (0.63)	39.2 (0.6)	5.3 (0.4)	33.9 (0.7)	95.4 (2.0)
Ser275	1.56 (0.71)	7.3 (0.3)	0.0 (0.2)	7.3 (0.3)	16.7 (0.8)
Asn278	2.02 (0.81)	32.7 (0.7)	6.4 (0.6)	26.3 (0.9)	67.6 (2.4)

Table 2. Continued

Interfacial Analysis - Monomer α					
Residue	$\Delta\Delta G_{\text{Binding}}$ (kcal/mol)	Average SASA _{Monomer} (%)	Average SASA _{Dimer} (%)	Average SASA _{Lost} (%)	Average SASA _{Lost} (\AA^2)
Tyr279	-0.02 (0.83)	3.7 (0.3)	0.3 (0.2)	3.4 (0.4)	11.3 (1.4)
Gln285	0.67 (0.75)	49.1 (0.9)	44.2 (1.2)	5.0 (1.5)	14.3 (4.2)
Tyr310	1.21 (0.82)	22.2 (0.7)	12.3 (0.6)	9.9 (0.9)	32.7 (3.1)
Asp317	0.76 (0.65)	22.8 (0.7)	13.8 (0.8)	8.9 (1.0)	22.3 (2.5)
Glu320	-0.62 (0.64)	11.3 (0.7)	5.9 (0.8)	5.4 (1.0)	14.8 (2.9)
Asp349	4.88 (0.64)	8.4 (0.5)	1.4 (0.4)	6.9 (0.6)	17.2 (1.5)
Thr350	0.23 (0.84)	42.7 (1.0)	24.9 (0.9)	17.8 (1.4)	43.6 (3.4)
Ile351	5.31 (1.28)	55.2 (0.5)	2.1 (0.5)	53.1 (0.7)	148.1 (1.9)
Arg352	6.35 (0.64)	34.6 (0.7)	4.3 (0.5)	30.3 (0.9)	103.1 (3.0)
Lys353	0.89 (0.63)	29.9 (1.2)	22.3 (0.8)	7.7 (1.4)	23.9 (4.5)
Glu354	5.71 (0.63)	35.5 (0.5)	4.5 (0.6)	31.0 (0.8)	85.9 (2.2)
Tyr355	5.17 (0.85)	40.5 (0.4)	4.1 (0.4)	36.4 (0.6)	120.8 (1.9)
Tyr358	17.34 (0.84)	40.7 (0.8)	6.8 (0.9)	34.0 (1.2)	113.0 (4.1)
Arg361	2.50 (0.64)	42.3 (1.5)	22.5 (1.6)	19.9 (2.2)	68.1 (7.4)
Ser362	-0.05 (0.70)	11.5 (0.9)	6.7 (0.6)	4.8 (1.0)	11.0 (2.4)
Ser365	0.29 (0.72)	36.9 (0.8)	31.7 (0.9)	5.2 (1.1)	11.7 (2.6)

^a Average solvent-accessible surface area (SASA) values for the residues in each amino acid position in monomer α . ^b Hot spots, grey and bold; warm spots, bold.

the backbone C_α atoms in the MD simulations of the FTase structure. In addition, this figure also shows the RMSd values for the subset of backbone atoms of the 111 interface amino acid residues that were the subject of more detail in this study. The results show that the system is well equilibrated after the initial 4 ns of simulation, particularly the interfacial amino acid residues. This was also confirmed through individual rms analysis of both monomers. Following this observation, the remaining 6 ns of simulation was taken into consideration for the ASM calculations and subsequent analysis.

2. Characterization of the Interface in FTase. From a structural point of view, FTase is a heterodimeric Zn enzyme, mainly composed of α -helices, that contains two very different subunits: subunit α and subunit β . Subunit α is composed of 377 amino acids^{63,64} disposed along 15 α -helices, encompassing seven successive pairs of coiled-coils (helices 2–15) that form an unusual double-layered, crescent-shaped, seven-helical hairpin domain, enveloping part of the β -subunit.^{71,142} The several helices are folded in such a way that all the helices in one layer are roughly parallel to each other and antiparallel to the helices in the adjacent layer⁷¹ (see Figure 1).

The β -subunit of FTase has a lower molecular mass than subunit α (46 kDa) but contains more amino acids: a total of 437.^{63,64} Composed of 14 α -helices, this subunit is arranged in an α - α barrel domain blocked at one end (by helix 14 β) and solvent-accessible at the other, consisting of a core of six parallel helices (3 β , 5 β , 7 β , 9 β , 11 β , and 13 β), which constitute the inner

portion of the barrel; and six peripheral helices (2 β , 4 β , 6 β , 8 β , 10 β , and 12 β), interconnecting the inner core helices and defining the outside of the helical barrel^{71,142} (see Figure 1). The peripheral helices are parallel to each other and antiparallel to the core helices.

In this enzyme, the active site Zn ion is located close to the interface of the two subunits at the top of the α - α barrel, in a junction between an interfacial hydrophilic surface groove that runs parallel to the rim of the α - α barrel, and an almost orthogonal deep cleft in the β -subunit formed by the central cavity of the barrel and lined with 10 highly conserved aromatic residues.^{71,142} The isoprenoid moiety of FPP binds in an extended conformation^{74,113} to this funnel-shaped hydrophobic cavity, with the diphosphate moiety packed in a positively charged cleft at the top of this cavity near the subunit interface and adjacent to the catalytic Zn ion.¹⁴² Zn is coordinated to the side chains of three residues from the β subunit: Asp297 β (mono or bidentate coordination),⁸³ Cys299 β , and His 362 β .

The α -subunit contacts the β -subunit barrel around half its circumference at the upper, open end of the barrel, an arrangement that places several residues from the α -subunit near the active-site Zn, forming part of the FPP binding site.¹⁴³ The α / β interface is defined by a total of 130 amino acid residues: 59 from the α -subunit and 71 from the β -subunit.

3. Analysis of the Energetic Contribution. In this study, we are interested in seeing how these effects can be translated in terms of energetic contribution to the dimerization of FTase.

Table 3. Differences in the Binding Free Energies ($\Delta\Delta G_{\text{Binding}}$) and Standard Deviation for the Wild Type FTase and Alanine Mutant Variants Calculated^a

Interfacial Analysis - Monomer β					
Residue	$\Delta\Delta G_{\text{Binding}}$ (kcal/mol)	SASA _{Monomer} (%)	SASA _{Dimer} (%)	SASA _{Lost} (%)	SASA _{Lost} (Å ²)
Tyr24	1.14 (1.07)	15.8 (1.4)	8.0 (0.8)	7.8 (1.6)	25.5 (5.3)
Gln36	-18.10 (0.81)	33.2 (1.3)	28.3 (1.2)	4.9 (1.8)	14.0 (5.1)
Asp37	-0.50 (0.61)	31.6 (0.6)	16.5 (0.9)	15.2 (1.1)	37.5 (2.7)
Asp38	-0.97 (0.60)	59.0 (0.5)	58.9 (0.6)	0.1 (0.8)	0.4 (1.9)
Val40	-2.45 (1.21)	39.8 (0.5)	17.3 (0.8)	22.5 (1.0)	57.3 (2.5)
Thr42	2.62 (1.06)	28.1 (0.4)	4.0 (0.3)	24.1 (0.5)	58.6 (1.1)
Thr44	1.38 (1.05)	14.1 (0.4)	1.0 (0.2)	13.1 (0.5)	31.5 (1.2)
Ser45	-0.29 (0.74)	10.3 (0.5)	6.9 (0.5)	3.4 (0.7)	7.5 (1.5)
Leu86	0.39 (1.27)	14.2 (0.6)	3.3 (0.5)	10.9 (0.7)	30.7 (2.1)
Arg87	1.95 (0.64)	45.5 (1.3)	21.7 (1.4)	23.8 (1.9)	78.9 (6.4)
Gln88	1.58 (0.79)	51.5 (1.1)	34.1 (1.0)	17.4 (1.5)	49.7 (4.4)
Leu89	-0.70 (1.26)	24.0 (0.6)	4.9 (0.5)	19.1 (0.8)	55.2 (2.2)
Asp91	2.45 (0.62)	52.0 (0.5)	39.4 (0.7)	12.6 (0.8)	31.0 (2.1)
Tyr93	-0.89 (1.07)	16.9 (1.1)	14.5 (1.1)	2.4 (1.5)	8.1 (5.0)
Glu94	4.28 (0.74)	48.6 (0.5)	11.9 (0.8)	36.7 (1.0)	102.0 (2.7)
Cys95	-0.20 (0.83)	43.4 (0.5)	23.6 (0.6)	19.8 (0.8)	47.8 (1.9)
Asp97	7.57 (0.59)	33.0 (0.4)	1.0 (0.2)	31.9 (0.5)	78.8 (1.2)
Arg100	1.62 (0.63)	19.1 (1.2)	2.1 (0.5)	17.0 (1.3)	60.4 (4.7)
Leu103	-0.38 (1.28)	9.7 (0.5)	0.8 (0.3)	8.8 (0.5)	25.2 (1.6)
Cys104	0.41 (0.83)	9.6 (0.4)	0.7 (0.3)	8.9 (0.5)	21.8 (1.2)
Asp125	2.52 (0.59)	26.8 (0.9)	6.7 (0.9)	20.2 (1.2)	49.1 (3.0)
Val126	-1.08 (1.19)	4.6 (0.3)	0.5 (0.2)	4.2 (0.4)	10.9 (0.9)
Phe129	-0.31 (1.27)	26.6 (1.3)	2.1 (0.4)	24.5 (1.4)	76.5 (4.3)
Leu132	1.12 (1.28)	40.0 (0.8)	21.4 (1.0)	18.5 (1.3)	52.5 (3.6)
Gln146	2.59 (0.82)	29.8 (0.5)	3.7 (0.4)	26.1 (0.7)	74.9 (2.0)
Tyr147	2.23 (1.07)	53.7 (0.8)	18.3 (1.1)	35.4 (1.3)	118.5 (4.3)
His149	-1.28 (0.74)	20.6 (0.5)	3.7 (0.5)	16.9 (0.7)	50.3 (2.1)
Met193	0.34 (1.21)	14.0 (0.9)	4.5 (0.6)	9.4 (1.1)	29.1 (3.4)
Glu198	6.09 (0.63)	41.7 (0.6)	5.4 (0.6)	36.3 (0.8)	99.0 (2.3)
Asn234	-0.60 (0.74)	10.8 (0.4)	9.6 (0.4)	1.1 (0.5)	2.9 (1.3)
Trp235	4.91 (1.25)	57.8 (0.6)	4.7 (0.6)	53.1 (0.8)	189.8 (2.9)
Glu236	6.45 (0.63)	9.4 (0.4)	0.5 (0.2)	8.9 (0.6)	24.7 (1.2)
Val242	1.58 (1.21)	33.7 (1.2)	16.1 (0.8)	17.6 (1.4)	44.6 (3.7)
Met245	9.15 (1.20)	39.1 (0.5)	0.70 (0.3)	38.4 (0.6)	113.7 (1.6)
Glu246	9.95 (0.63)	22.2 (0.5)	0.2 (0.3)	22.0 (0.6)	59.0 (1.5)
His248	0.75 (0.74)	18.3 (0.8)	13.4 (0.7)	4.9 (1.1)	14.2 (3.1)
Tyr251	0.80 (1.07)	22.2 (0.8)	9.7 (0.7)	12.4 (1.1)	40.6 (3.5)

Table 3. Continued

Interfacial Analysis - Monomer β					
Residue	$\Delta\Delta G_{\text{Binding}}$ (kcal/mol)	Average SASA _{Monomer} (%)	Average SASA _{Dimer} (%)	Average SASA _{Lost} (%)	Average SASA _{Lost} (\AA^2)
Lys271	2.27 (0.73)	49.3 (1.6)	22.8 (0.9)	26.5 (1.9)	84.6 (6.0)
Leu274	0.94 (1.27)	14.3 (0.6)	2.0 (0.4)	12.3 (0.7)	34.7 (2.0)
Gln275	1.81 (0.82)	41.5 (0.8)	14.9 (0.7)	26.6 (1.0)	74.4 (2.9)
Thr278	3.24 (1.09)	16.6 (0.6)	2.4 (0.2)	14.2 (0.6)	34.6 (1.5)
Ser279	-0.17 (0.72)	23.5 (0.3)	7.7 (0.4)	15.8 (0.5)	34.7 (1.1)
Arg280	5.36 (0.63)	6.8 (0.3)	0.9 (0.2)	6.0 (0.4)	19.6 (1.3)
Gln281	4.96 (0.79)	11.4 (0.3)	1.0 (0.3)	10.4 (0.4)	30.4 (1.2)
Met282	-0.05 (1.22)	4.9 (0.5)	3.0 (0.4)	1.8 (0.7)	5.3 (1.9)
Arg283	9.33 (0.65)	44.1 (0.6)	10.8 (0.6)	33.3 (0.9)	115.7 (3.1)
Arg291	0.22 (0.63)	25.0 (0.6)	5.9 (0.5)	19.1 (0.7)	66.1 (2.6)
Cys292	0.71 (0.83)	24.3 (0.4)	0.6 (0.2)	23.7 (0.4)	57.8 (1.0)
Asn293	2.14 (0.75)	44.9 (0.5)	2.8 (0.3)	42.1 (0.6)	109.9 (1.5)
Lys294	1.32 (0.71)	22.3 (0.6)	17.0 (0.6)	5.3 (0.8)	17.4 (2.6)
Leu315	-0.32 (1.27)	9.2 (0.8)	5.4 (0.6)	3.8 (1.0)	10.7 (2.9)
Asp320	-0.69 (0.62)	18.6 (0.8)	12.1 (0.8)	6.6 (1.1)	16.1 (2.7)
Leu323	3.64 (1.26)	12.8 (0.8)	10.6 (0.8)	2.2 (1.1)	6.4 (2.7)
Ser324	-0.44 (0.74)	13.2 (0.8)	4.0 (0.6)	9.3 (1.0)	20.5 (2.2)
His327	3.06 (0.75)	27.0 (0.8)	17.5 (0.9)	9.6 (1.2)	28.0 (3.5)
Trp328	-0.67 (1.29)	1.2 (0.4)	0.6 (0.4)	0.6 (0.6)	2.2 (2.0)
Met329	4.18 (0.99)	13.8 (0.8)	1.7 (0.4)	12.2 (0.9)	35.5 (2.7)
His331	2.22 (0.74)	32.1 (0.8)	11.4 (0.7)	20.7 (1.0)	61.5 (3.1)

^a Average Solvent Accessible Surface Area (SASA) values for the residues in each amino acid position in monomer β . Hot spots, grey and bold; warm spots, bold.

The values of $\Delta\Delta G_{\text{binding}}$ calculated from the ASM studies allow us to identify the amino acid residues that contribute the most to the binding of the two monomers in FTase. Because these amino acid residues are determinant to the binding of the two monomers, the development of drugs that are able to prevent their interaction could avoid dimer formation, constituting an alternative strategy to inhibit FTase enzymatic activity. Such critical amino acid residues are called hot spots. A hot spot is an amino acid residue with a $\Delta\Delta G_{\text{binding}}$ value higher than 4 kcal/mol. The amino acids with a $\Delta\Delta G_{\text{binding}}$ value between 2 and 4 kcal/mol are less important but still vital to the binding process and are designated as warm spots.

From the 130 interface residues considered, a total of 24 hot spots (18.4%), 25 warm spots (19.2%), and 62 null spots (47.7%) were identified. Nineteen interfacial amino acid residues (the glycines, alanines, and prolines) were not evaluated because of the intrinsic limitations of the ASM method, as justified in the Methods section. From the 53 α -subunit interface residues evaluated with ASM, we have identified 13 hot spots and 14 warm

spots, with averages in free energy differences of 8.11 and 2.93 kcal/mol, respectively (Table 1). From the 58 β -subunit interface residues studied with ASM, we have identified 11 hot spots and 11 warm spots, with averages in free energy differences of 6.57 and 2.63 kcal/mol, respectively (Table 1).

Table 2 summarizes the computational ASM results for all the interface amino acid residues in the α -subunit of FTase; Table 3 presents the same information but for the β -subunit. The results indicate Tyr358 α , Asn238 α , Glu274 α , Val88 α , and Tyr200 α as the residues in the α -subunit that contribute the most for dimer formation among a total of 13 hot spots identified, whereas in the β -subunit, Glu246 β , Arg283 β , Met245 β , and Asp97 β are the most important hot spots identified from a total of 11 residues with a contribution higher than 4 kcal/mol for dimer formation.

Figure 3 illustrates all the hot spots identified in the α -subunit, while offering also a view of the position of the most relevant warm spots and the interaction of the hot spots and warm spots at the α -subunit with the β -subunit. The results presented in Figure 3 show that the α -subunit hot spots are concentrated mainly in two

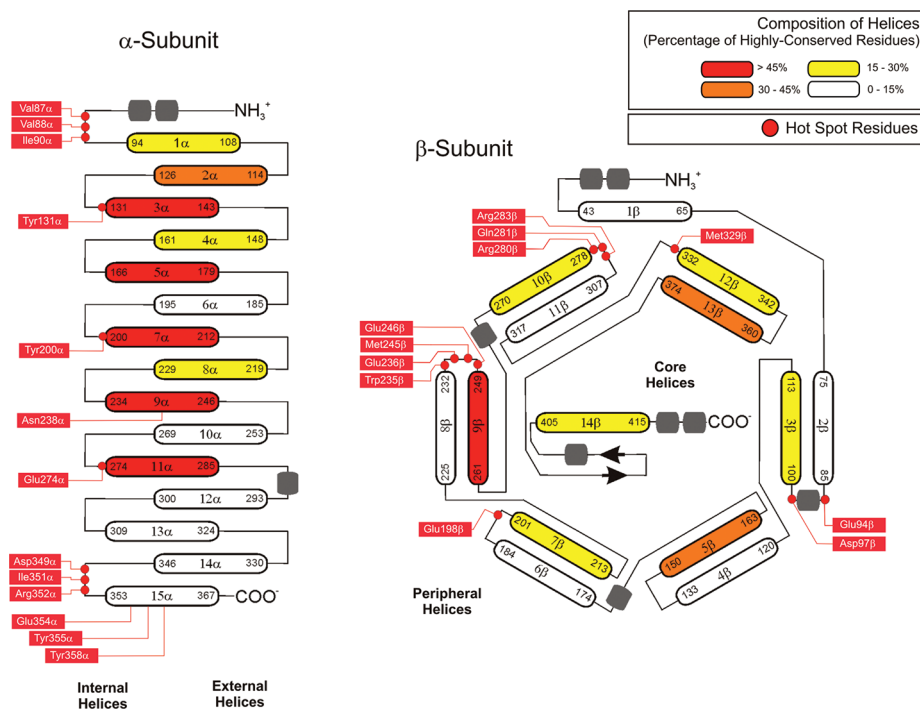


Figure 2. Schematic representation of the topology of subunits α and β in FTase, indicating the several helices, the percentage of highly conserved residues that constitute each helix, and the hot spots identified in this study. Highly conserved residues are those with a conservation score of 7 or higher, on a 1–9 scale (9 conserved and 1 variable).¹³⁸ In the helices, the numbers indicated represent the initial and final residues.

regions at the interior extremities of its double-layered, crescent-shaped domain. One of these regions (region A1) is defined by the hot spot residues Val87 α , Val88 α , Ile90 α , and Tyr131 α and by the warm spots His135 α and Thr132 α and establishes important interactions with helices 3 β , 4 β , 5 β , and 6 β . The other region (region A2) is defined by the hot spots Asp349 α , Ile351 α , Arg352 α , Glu354 α , Tyr355 α , and Tyr358 α and by the warm spot Arg361 α and interacts with helices 10 β and 11 β . This region differs from the first in that it contains a very significant number of charged amino acid residues (four out of seven). Only three hot spots in the α -subunit were identified outside of these two regions, occupying a more central position at the α/β interface (Tyr200 α , Asn238 α , and Glu274 α), although not close together.

Figure 4 shows the position of the several hot spots and warm spots identified in the β subunit, displaying also their interaction with the α -subunit. The results presented in Figure 4 also show a concentration of hot spots in three regions of the β -subunit. Two of these regions are in opposing extremities of the $\alpha-\alpha$ barrel domain that comprises most of the β -subunit, whereas the third one occupies a more central position. Interestingly, the two regions in opposing extremities of the β -subunit interact directly with the two important regions previously identified in opposing extremities of the α -subunit (regions A1 and A2).

The first region identified in the β -subunit (region B1) contains a large amount of charged residues and encompasses the hot spots Glu94 β and Asp97 β and the warm spots Asp91 β , Asp125 β , Gln146 β , and Tyr147 β . It interacts with helices 1 α and 3 α and with region A1 defined by the hot spots Val87 α , Val88 α , Ile90 α , and Tyr131 α in the α -subunit. The second region (region B2), which occupies the opposite side of the barrel, contains the hot spots Arg280 β , Gln28 β , Arg283 β , and Met329 β , together with several warm spots (see Figure 4), and

interacts with the α -subunit at helices 13 α and 15 α and with the A2 hot spot region. Finally, the third region (region B3) contains the hot spots Glu198 β , Trp235 β , Glu236 β , Met245 β , and Glu246 β and interacts with the α -subunit at a more central position of its double-layered crescent-shaped domain, particularly with helices 7 α , 9 α , and 11 α and with hot spots Tyr200 α , Asn238 α , and Glu274 α .

Interestingly, from Figure 2, which presents a schematic view on the overall topology of the α and β -subunits and of the relative position of the hot spots identified, it can be observed that the great majority of the hot spots identified (83%) are not located in helices, but are present in the structurally more disordered regions connecting different helices. The exceptions are Asn238 α (present in helix 9 α) and Glu354 α , Tyr355 α , and Tyr358 α (present in helix 15 α).

4. Relation with Typical Statistical Hot Spot Preferences.

A systematic study⁹⁷ analyzing a total of 2325 alanine mutants for which the change in the free energy of binding upon mutation to alanine had been experimentally measured, has identified tryptophan, tyrosine, arginine, isoleucine, aspartate and glutamate as the most common residues present among those contributing more to the $\Delta\Delta G_{\text{binding}}$. These general trends are in agreement with tryptophan Trp235 β ; tyrosines Tyr131 α , Tyr200 α , Tyr355 α , and Tyr358 α ; arginines Arg352 α , Arg280 β , and Arg283 β ; isoleucines Ile90 α and Ile351 α ; aspartate Asp349 α and Asp97 β ; asparagine Asn238 α ; and glutamates Glu274 α , Glu354 α , Glu94 β , Glu198 β , Glu236 β , and Glu246 β as hot spots in FTase.

Valines, such as Val87 α and Val88 α , however, are rather uncommon among hot spots and warm spots, with the above-mentioned study having identified no valine residues contributing more than 2 kcal/mol to $\Delta\Delta G_{\text{binding}}$ among a total of 107 valine–alanine mutants considered. According to the same study,⁹⁷ methionines and glutamines are also rather uncommon as hot spots or warm

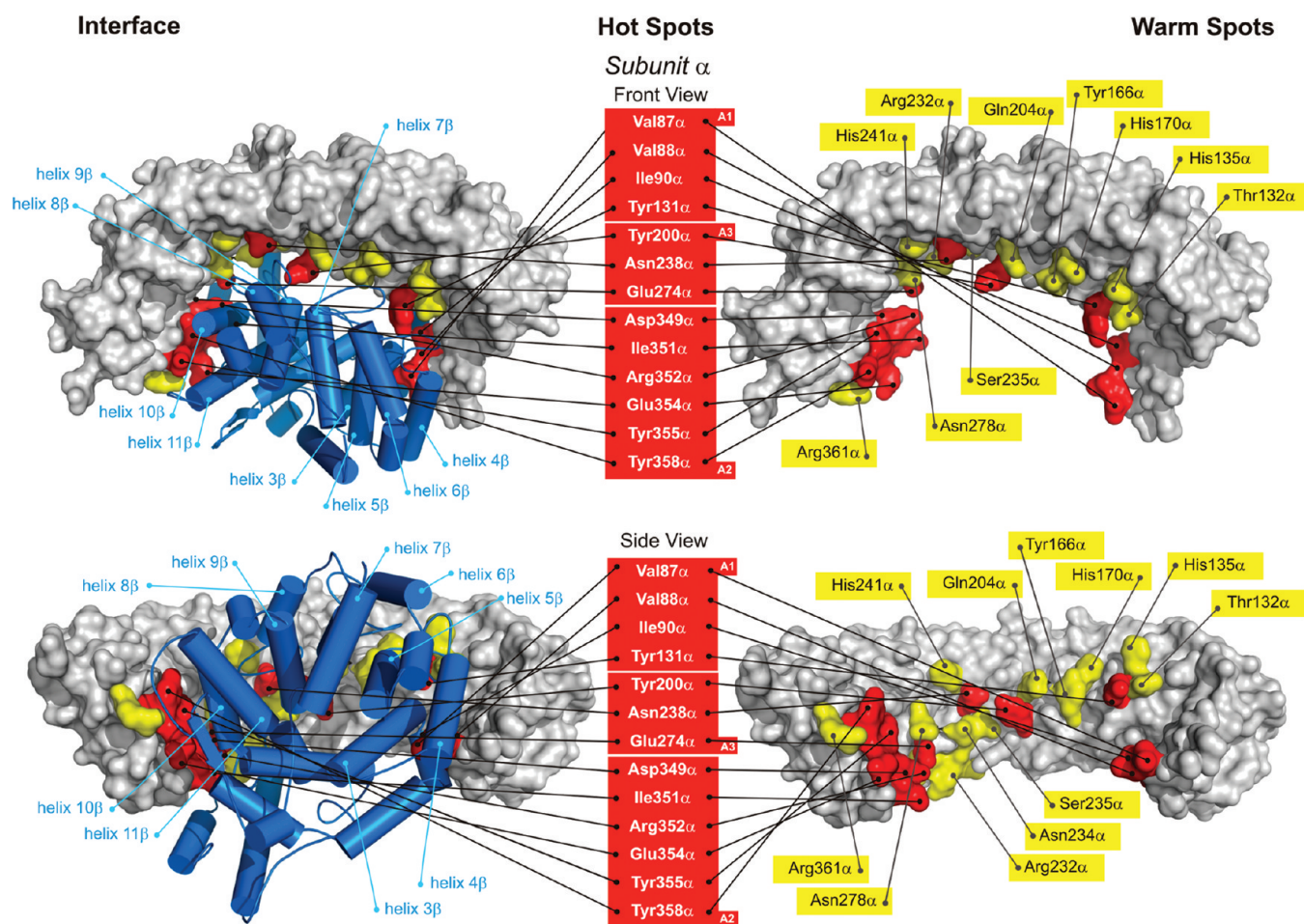


Figure 3. Schematic representation of the hot spots and warm spots in the α -subunit of FTase and of their interaction with the β -subunit.

spots, with only 2 Met and 5 Gln identified in a total of 69 methionine–alanine mutants and 160 glutamine–alanine mutants. The unusually high energetic contribution calculated in this study for Val87 α and Val88 α , Met245 β , Met329 β , and Gln281 β could be a distinctive characteristic of FTase, which could be worth exploring in future studies.

5. Energy Decomposition in Hot Spot Residues. Table 4 presents the energetic contribution of all the individual components to the differences in the binding free energies ($\Delta\Delta G_{\text{Binding}}$) between the wild-type FTase and alanine mutant variants for the hot spots. The components presented include the electrostatic energy term ($\Delta\Delta E_{\text{electrostatic}}$), the van der Waals energy term ($\Delta\Delta E_{\text{vdW}}$), and the polar ($\Delta\Delta G_{\text{PolarSolv}}$) and nonpolar ($\Delta\Delta G_{\text{NonPolarSolv}}$) contributions to the solvation free energy. The two columns referring to the hydrophilic and hydrophobic contributions represent, respectively, the sum of the electrostatic energy term and the polar contribution to the solvation free energy (hydrophilic contribution) and of the van der Waals and nonpolar contribution to the solvation free energy (hydrophobic contribution).

For most of the hot spots identified, the hydrophobic contribution to the $\Delta\Delta G_{\text{Binding}}$ upon alanine mutation are dominant in relation to the hydrophilic contributions, demonstrating the importance of this type of interaction in FTase dimer formation. The results presented in Table 4 highlight the rather high hydrophilic contribution to the differences in the binding free energies for the mutations Asn238 α , Tyr358 α , Glu274 α , Glu246 β ,

and Arg280 β . The last three residues are charged. Hence, their mutation to alanine with a substantial change in the electrostatic energy term ($\Delta\Delta E_{\text{electrostatic}}$) partially compensated by an opposite change in the polar contribution to the solvation free energy ($\Delta\Delta G_{\text{PolarSolv}}$) is not unexpected. Asn238 α and Tyr358 α , however, two polar but uncharged amino acid residues, display a distinct trend with an unusually high polar contribution to the solvation free energy ($\Delta\Delta G_{\text{PolarSolv}}$).

The results presented in Table 4 show the existence of clear differences between the several hot spot regions identified on the FTase's interface. Regions A1, A2, and the remaining hot spots in the α -subunit have average electrostatic energy ($\Delta\Delta E_{\text{electrostatic}}$) contributions of 2.03, 0.46, and 2.89 kcal/mol. Regions B1 and B3 have negative contributions to $\Delta\Delta E_{\text{electrostatic}}$ (−8.34 and −4.52 kcal/mol, on average), whereas B2 has a strong positive contribution (13.11 kcal/mol). These trends reflect the electrostatic nature of the several regions, with A1 and A3 being composed of mainly hydrophobic amino acid residues, A2 containing several charged residues but being mainly nonpolar, B1 being negatively charged, B3 having an excess of negative charge, and B2 having a clear excess of positive charge. Average values of $\Delta\Delta E_{\text{vdW}}$ and $\Delta\Delta G_{\text{NonPolarSolv}}$ are quite similar between regions, and the $\Delta\Delta G_{\text{PolarSolv}}$ average contributions are in line with the observations reported for $\Delta\Delta E_{\text{electrostatic}}$.

6. SASA Analysis. Bogan and Thorn⁹⁷ in their seminal work “Anatomy of Hot-spots in Protein Interfaces” have found the

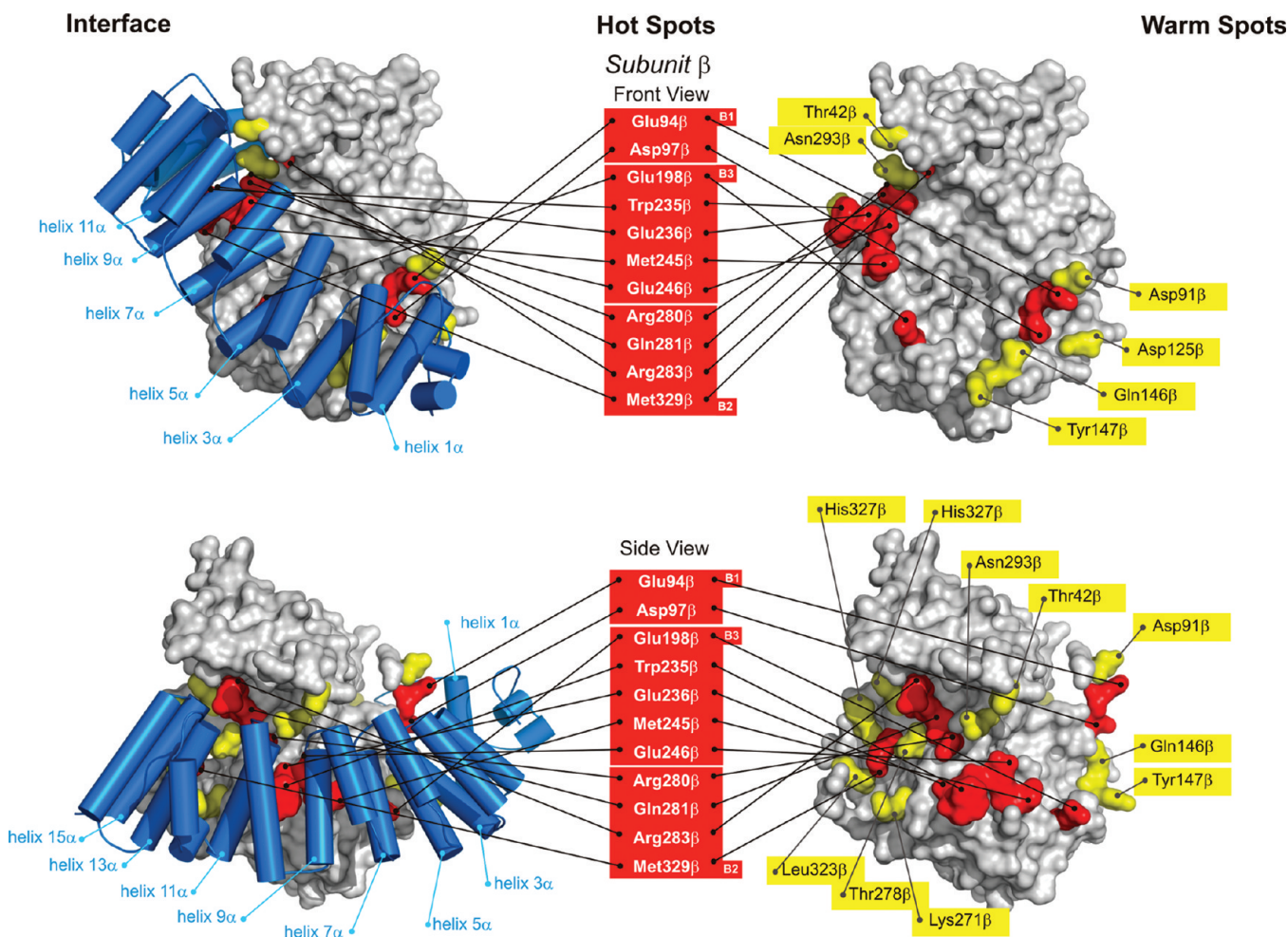


Figure 4. Schematic representation of the hot spots and warm spots in the β -subunit of FTase and of their interaction with the α -subunit.

existence of very little correlation between the buried surface area and the free energy of binding and have concluded that the occlusion from solvent in the protein–protein complexes is a necessary, although not sufficient, requirement for the occurrence of hot spots. To evaluate these features, we have complemented the energetic analysis performed above for all the interfacial amino acid residues (in terms of calculated $\Delta\Delta G_{\text{binding}}$ values) with solvent accessible surface area calculations for all the interfacial amino acid residues in an attempt to correlate the energetic contribution of each amino acid residue with its solvent accessibility in the FTase complex.

These values are presented in Tables 2 and 3 and include the solvent-accessible surface area (SASA) values calculated for each residue, considering the full dimer ($\text{SASA}_{\text{dimer}}$) and considering only the residues in the same subunit of each residue ($\text{SASA}_{\text{monomer}}$). Given the large difference in size that characterizes the different amino acid residues present at the interface, these values are presented as a percentage of the potential SASA for the free residue.

In the convention used in this study, a high $\text{SASA}_{\text{monomer}}$ indicates that a given residue is poorly shielded by residues from its own subunit and exposed to the solvent or to residues from the other subunit, whereas a low $\text{SASA}_{\text{monomer}}$ indicates a residue that is highly protected from other interactions by residues of its own subunit. Analogously, a high $\text{SASA}_{\text{dimer}}$ illustrates that in the dimer, a given residue is very much exposed to the solvent, whereas a

low $\text{SASA}_{\text{dimer}}$ indicates a residue extremely protected by residues from the two subunits. From the difference between $\text{SASA}_{\text{dimer}}$ and $\text{SASA}_{\text{monomer}}$ (described as SASA lost upon dimerization), it is possible to get an idea of the contribution in terms of interaction surface area of each residue to the subunit interface (values expressed in percentage and in area).

Average SASA values are also presented in Table 1 for hot spots, warm spots, and null spots identified. Hot spots clearly have a higher SASA when considering residues only from their own subunit ($\text{SASA}_{\text{monomer}}$), with 35.3% of their potential surface area free for interaction with the other subunit or with solvent molecules, a value that decreases to 3.5% for the dimer (average decrease of 93.5 \AA^2 per residue). In particular, the hot spots Val87 α , Val88 α , Asp97 β , Glu236 β , Met245 β , Glu246 β , Arg280 β , and Gln281 β have average $\text{SASA}_{\text{dimer}}$ values of 1.0% or below, with Val88 α , Tyr131 α , Tyr200 α , Ile351 α , Tyr355 α , and Trp235 β having values of SASA lost upon dimerization higher than 120.0 \AA^2 .

Warm spots are less exposed when considering only the monomer (30.0%), and upon dimer formation, the corresponding SASA decreases to 9.7%, which represents an average decrease of 58.1 \AA^2 (21%) per amino acid residue (maximums Arg232 α with 146.5 \AA^2 and Tyr147 β with 118.5 \AA^2 decreases). Null spots interact preferentially with their own subunit, exhibiting an average $\text{SASA}_{\text{monomer}}$ of only 25.2%, a value that decreases

Table 4. Energetic Contribution and Standard Deviation of All the Individual Components to the Differences in the Binding Free Energies ($\Delta\Delta G_{\text{Binding}}$) between the Wild Type FTase and Alanine Mutant Variants for the Hot Spots Identified in FTase

region	residue	$\Delta\Delta E_{\text{electrostatic}}$ (kcal/mol)	$\Delta\Delta E_{\text{vdW}}$ (kcal/mol)	$\Delta\Delta G_{\text{NonPolarSolv}}$ (kcal/mol)	$\Delta\Delta G_{\text{PolarSolv}}$ (kcal/mol)	hydrophilic contribution (kcal/mol)	hydrophobic contribution (kcal/mol)	$\Delta\Delta G_{\text{Binding}}$ (kcal/mol)
A1	Val87 α	1.86 (1.15)	5.47 (0.32)	0.15 (0.02)	-0.78 (1.68)	1.08 (2.03)	5.62 (0.32)	6.70 (1.29)
	Val88 α	2.18 (1.17)	5.80 (0.32)	0.24 (0.02)	-0.02 (1.68)	2.16 (2.03)	6.04 (0.32)	8.19 (1.26)
	Ile90 α	0.64 (1.18)	7.18 (0.32)	0.25 (0.02)	-1.65 (1.68)	-1.01 (2.05)	7.43 (0.32)	6.41 (1.28)
	Tyr131 α	3.45 (1.00)	9.31 (0.32)	0.53 (0.02)	-7.08 (1.68)	-3.63 (1.47)	9.84 (0.32)	6.21 (0.84)
	average	2.03	6.94	0.29	-2.38	-0.35	7.23	6.88
A3	Tyr200 α	3.79 (0.79)	11.94 (0.32)	0.65 (0.02)	-8.21 (1.07)	-4.42 (1.33)	12.59 (0.32)	8.17 (0.83)
	Asn238 α	1.83 (0.78)	4.24 (0.32)	0.08 (0.02)	9.46 (1.07)	11.29 (1.33)	4.32 (0.32)	15.61 (0.83)
	Glu274 α	3.05 (0.49)	2.51 (0.32)	0.19 (0.02)	3.70 (0.89)	6.75 (1.02)	2.70 (0.33)	9.44 (0.63)
	average	2.89	6.23	0.31	1.65	4.54	6.54	11.07
A2	Asp349 α	-2.74 (0.53)	0.97 (0.32)	-0.04 (0.02)	6.68 (0.75)	3.94 (0.92)	0.93 (0.32)	4.88 (0.64)
	Ile351 α	-0.30 (1.18)	7.40 (0.32)	0.41 (0.02)	-2.19 (1.68)	-2.49 (2.05)	7.81 (0.33)	5.31 (1.28)
	Arg352 α	13.10 (0.58)	7.58 (0.32)	0.31 (0.02)	-14.63 (0.79)	-1.53 (0.98)	7.89 (0.33)	6.35 (0.64)
	Glu354 α	-8.17 (0.58)	3.82 (0.32)	0.10 (0.02)	9.96 (0.77)	1.79 (0.96)	3.92 (0.32)	5.71 (0.63)
	Tyr355 α	-0.26 (0.78)	8.14 (0.32)	0.48 (0.02)	-3.19 (1.08)	-3.45 (1.33)	8.62 (0.32)	5.17 (0.85)
	Tyr358 α	1.15 (0.78)	7.37 (0.32)	0.63 (0.02)	8.19 (1.07)	9.34 (1.33)	8.00 (0.32)	17.34 (0.84)
B1	Glu94 β	-11.07 (0.58)	4.47 (0.32)	0.38 (0.02)	10.49 (1.31)	-0.58 (1.44)	4.85 (0.32)	4.28 (0.74)
	Asp97 β	-5.61 (0.58)	2.62 (0.32)	0.13 (0.02)	10.43 (1.28)	4.82 (1.41)	2.75 (0.32)	7.57 (0.59)
	average	-8.34	3.55	0.26	10.46	2.12	3.80	5.93
B3	Glu198 β	2.40 (0.58)	1.74 (0.32)	0.30 (0.02)	1.65 (1.31)	4.05 (1.43)	2.04 (0.32)	6.09 (0.63)
	Trp235 β	0.51 (1.18)	14.27 (0.32)	0.56 (0.02)	-10.41 (1.41)	-9.90 (1.83)	14.83 (0.32)	4.91 (1.25)
	Glu236 β	-16.15 (0.49)	2.52 (0.32)	0.00 (0.02)	20.08 (0.94)	3.93 (1.06)	2.52 (0.32)	6.45 (0.63)
	Met245 β	-0.64 (1.00)	8.49 (0.32)	0.34 (0.02)	0.97 (1.07)	0.33 (1.47)	8.83 (0.32)	9.15 (1.20)
	Glu246 β	-8.74 (0.58)	3.35 (0.32)	-0.09 (0.02)	15.43 (0.73)	6.69 (0.93)	3.26 (0.32)	9.95 (0.63)
	average	-4.52	6.07	0.22	5.54	1.02	6.30	7.31
B2	Arg280 β	27.73 (0.59)	0.32 (0.32)	0.03 (0.02)	-22.72 (0.75)	5.01 (0.95)	0.35 (0.32)	5.36 (0.63)
	Gln281 β	-0.16 (0.79)	2.10 (0.32)	-0.10 (0.02)	3.12 (1.41)	2.96 (1.61)	2.00 (0.32)	4.96 (0.79)
	Arg283 β	24.35 (0.60)	6.55 (0.32)	0.69 (0.02)	-22.26 (0.79)	2.09 (0.99)	7.24 (0.32)	9.33 (0.65)
	Met329 β	0.53 (1.00)	1.86 (0.32)	0.02 (0.02)	1.78 (0.77)	2.31 (1.26)	1.88 (0.32)	4.18 (0.99)
	average	13.11	2.71	0.16	-10.02	3.09	2.87	5.96

only slightly when considering the dimer, representing an average drop of 34.0 Å² of the potential amino acid SASA (12.1%).

7. Hydrogen Bonding Analysis. At this time, it is pertinent to show the principal hydrogen bonds established in the FTase interface. Hydrogen bonds seam the monomers together to form a stable dimer. We have performed a hydrogen bonding analysis of all the interactions between residues from the two monomers. Table 5 presents the FTase interface hydrogen bonds that are resident for more than 40% of the MD simulation, their percentage of occupancy, the average hydrogen bonding distance between the two heavy atoms involved, the average lifetime, and the maximal occupancy over the period of MD simulation considered.

There are 21 hydrogen bonds between the FTase monomers that are present during more than 40% of the MD simulation. It can be observed that the hydrogen bonds involve at least one hot spot or warm spot in 95% of the cases (20 hydrogen bonds).

Just one hydrogen bond, between the residues Lys198 α and Arg291 β , does not involve a warm spot or a hot spot.

The top 2 hydrogen bonds (Glu246 β –Ser235 α , Glu246 β –Asn238 α), with percentages of occupation higher than 80%, involve the same hot spot from the β monomer and two different warm spots from the α monomer. Between the hot spot Glu198 β and the null spot Arg173 α is also established an important hydrogen bond (the third of the table). Particularly important are the hydrogen bonds established between hot spots Glu281 β –Arg352 α , Glu274 α –Gln281 β , Glu274 α –Arg280 β , Glu246 β –Tyr200 α , and Glu274 α –Arg280 β . Across the interface, the hydrogen bonds mentioned in this paragraph can also be considered as particularly important targets for the inhibition of dimer formation.

In Table 5, the residues identified with an asterisk are not interface residues, but residues that establish important hydrogen bonds with the interface residues as a result of their proximity and charge complementariness. For example, the residue Lys348 α is

Table 5. FTase Interface Hydrogen Bonds That Are Resident for More than 40% of the MD Simulation, Their Percentage of Occupancy, the Average Hydrogen Bond Distance between the Two Heavy Atoms Involved, the Average Lifetime, and the Maximum Occupancy over the Period of 10 ns Simulation

DONOR		ACCEPTOR			%Occupation	Average distance ¹ (Å)	Average Lifetime (ps)	Maximal Occupancy (ps)
residue	atom	residue	atom1	atom2				
Glu246β	OE2	Ser235α	HG	OG	88.57	2.67 (0.12)	41.2	170
Glu246β	OE1	Asn234α	HD22	ND2	80.13	2.82 (0.09)	17.7	55
Glu198β	OE2	Arg173α	HH22	NH2	78.03	2.81(0.09)	10	34
Gln48β*	OE1	Arg232α	HH12	NH1	70.20	2.83 (0.09)	7.1	18
Arg104α								
Gln146β	OE1	*	HH21	NH2	68.93	2.85 (0.09)	6.7	24
Arg104α								
Asp97β	OD1	*	HH12	NH1	67.10	2.83 (0.09)	7.1	39
Tyr147β	O	Tyr131α	HH	OH	66.43	2.81 (0.11)	6.1	16
Arg104α								
Asp97β	O	*	HH22	NH2	65.57	2.84 (0.09)	6.3	30
Asn273α	OD1	Asn293β	HD21	ND2	55.53	2.86 (0.08)	4.7	13
Gln281β	O	Arg352α	HE	NE	55.43	2.86 (0.08)	4.9	22
Glu274α	OE2	Gln281β	HH22	NH2	53.33	2.81 (0.09)	15.4	39
Lys348α*	O	Arg283β	HH12	NH1	52.6	2.86 (0.09)	4.6	16
Glu274α	OE1	Arg280β	HH12	NH1	52.47	2.84 (0.09)	5.7	21
Lys198α	O	Arg291β	HH22	NH2	52.33	2.86 (0.08)	4.5	12
Gly244β?	O	Asn238α	HD21	ND2	49.43	2.88 (0.08)	4.1	11
Glu246β	O	Tyr200α	HH	OH	49.30	2.83 (0.11)	4.1	15
Glu198β	OE1	Arg173α	HH12	NH1	48.67	2.84 (0.09)	5.3	22
Ser275α	OG	Asn293β	HD22	ND2	47.30	2.87 (0.08)	4.3	12
Glu274α	OE2	Arg280β	HH12	NH1	43.73	2.85 (0.09)	4.7	19
Arg104α								
Gln146β	OE1	*	HE	NE	41.10	2.87 (0.08)	3.8	22
Ser279β	O	Arg352α	HH21	NH2	40.13	2.83 (0.09)	5.0	15

^a The hot spots and warm spots are colored in red and yellow, respectively. The residues with an asterisk (*) are residues very close to the interface, establishing important interactions with the interface residues, but that do not establish significant van der Waals contact.

not a hot spot, but the oxygen of the main chain establishes an important interaction with the hot spot residue Arg283β.

The residue Gly244β is an interface residue that establishes an important hydrogen bond with the hot spot residue Asn238α; however, it was not identified as a hot, warm, null spot (glycines cannot be studied with ASM and are not common hot

spots; however, SASA indicates a small exposure to the solvent when the dimer is formed). Globally, these results provide an atomic level explanation for the energetic trend observed from the computational ASM results, showing the importance of the hydrogen bonds formed in the energetic contribution that each residue makes for dimer formation.

■ CONCLUSIONS

In this study, we have presented a detailed atomistic analysis of the subunit interface in the enzyme FTase, an important pharmacological target for the development of new drugs. In particular, we have evaluated the energetic contribution of all the amino acid residues at the subunit interface of this heterodimeric enzyme in an attempt to identify all the most important determinants for dimer formation. This analysis was further complemented with a dynamic analysis of all the hydrogen bonds formed between the two subunits and of the solvent accessible surface areas of all the interfacial amino acid residues, providing important clues for the development of new farnesyltransferase inhibitors designed to block the association of the two subunits, thereby preventing the formation of the fully active FTase form.

The ASM results highlighted the particular importance of a set of 24 amino acid residues for dimer formation. Thirteen of these residues are included in the α -subunit, and 11 are part of the β -subunit. From these, the most important contributions are made by residues Tyr358 α , Asn238 α , Glu274 α , Val88 α , Tyr200 α , Glu246 β , Arg283 β , and Met245 β . Mutating one of these residues by alanine leads to a destabilization of the resulting formed dimer of more than 8 kcal/mol when comparing with the wild type FTase. Interestingly, 83% of the hot spots identified are located in the more disordered regions connecting different helices and not on the many α -helices (a total of 29 helices) that constitute the enzyme.

In general, the hot spots identified have also been shown to be the largest contributors, in terms of area, to the subunit of the dimer, with each one of the hot spots identified losing, on average, 93.5 Å² of solvent-accessible surface area upon dimer formation. Interestingly, the hot spots from the α subunit have been shown to have a higher average contribution to the formation of the dimer than those of the β subunit (8.11 kcal/mol and 105.9 Å² of SASA lost in the α subunit against 6.57 kcal/mol and 105.9 Å² in the β subunit).

This study also shows that all the most important hydrogen bonds between residues from different subunits involve hot spot or warm spot residues Glu246 β , Asp97 β , Tyr131 α , Gln281 β , and Arg352 α .

Inhibitors designed to bind the residues identified in this study as hot spots or warm spots or to interfere or disrupt the more relevant and persistent hydrogen bonds observed in the course of the MD simulations are much more likely to have a greater effect on blocking the formation of the fully active FTase form. These features should be taken into account in future drug design and development studies targeting this important enzyme.

■ AUTHOR INFORMATION

Corresponding Author

*E-mail: mjraramos@fc.up.pt.

■ ACKNOWLEDGMENT

This work has been supported by Fundação para a Ciência e a Tecnologia (FCT) through Grant No. PEst-C/EQB/LA0006/2011. Marta A. S. Perez thanks FCT for a Ph.D. grant (SFRH/BD/43600/2008).

■ REFERENCES

- (1) Cox, A. D.; Der, C. J. *Curr. Opin. Pharmacol.* **2002**, *2*, 388–393.
- (2) Doll, R. J.; Kirschmeier, P.; Bishop, W. R. *Curr. Opin. Drug Discovery Dev.* **2004**, *7*, 478–486.
- (3) Rowinsky, E. K. *J. Clin. Oncol.* **2006**, *24*, 2981–2984.
- (4) Puntambekar, D. S.; Giridhar, R.; Yadav, M. R. *J. Enzyme Inhib. Med. Chem.* **2007**, *22*, 127–140.
- (5) Hancock, J. F.; Magee, A. I.; Childs, J. E.; Marshall, C. J. *Cell* **1989**, *57*, 1167–1177.
- (6) Jackson, J. H.; Cochrane, C. G.; Bourne, J. R.; Solski, P. A.; Buss, J. E.; Der, C. J. *Proc. Natl. Acad. Sci. U.S.A.* **1990**, *87*, 3042–3046.
- (7) Kato, K.; Cox, A. D.; Hisaka, M. M.; Graham, S. M.; Buss, J. E.; Der, C. J. *Proc. Natl. Acad. Sci. U.S.A.* **1992**, *89*, 6403–6407.
- (8) Dolence, J. M.; Poulter, C. D. *Proc. Natl. Acad. Sci. U.S.A.* **1995**, *92*, 5008–5011.
- (9) James, G.; Goldstein, J. L.; Brown, M. S. *Proc. Natl. Acad. Sci. U.S.A.* **1996**, *93*, 4454–4458.
- (10) Takai, Y.; Sasaki, T.; Matozaki, T. *Physiol. Rev.* **2001**, *81*, 153–208.
- (11) Ayral-Kaloustian, S.; Salaski, E. *J. Curr. Med. Chem.* **2002**, *9*, 1003–1032.
- (12) Ohkanda, J.; Knowles, D. B.; Blaskovich, M. A.; Sefti, S. M.; Hamilton, A. D. *Curr. Top. Med. Chem.* **2002**, *2*, 303–323.
- (13) Brunner, T. B.; Hahn, S. M.; Gupta, A. K.; Muschel, R. J.; McKenna, W. G.; Bernhard, E. J. *Cancer Res.* **2003**, *63*, 5656–5668.
- (14) Caponigro, F.; Casale, M.; Bryce, J. *Expert Opin. Invest. Drugs* **2003**, *12*, 943–954.
- (15) Adjei, A. A. *Cancer Chemother. Biol. Response Modif.* **2005**, *22*, 123–133.
- (16) Kurzrock, R. *Clin. Adv. Hematol. Oncol.* **2005**, *3*, 161–162.
- (17) Appels, N. M. G. M.; Beijnen, J. H.; Schellens, J. H. M. *Oncologist* **2005**, *10*, 565–578.
- (18) Basso, A. D.; Kirschmeier, P.; Bishop, W. R. *J. Lipid Res.* **2006**, *47*, 15–31.
- (19) Sousa, S. F.; Fernandes, P. A.; Ramos, M. J. *Curr. Med. Chem.* **2008**, *15*, 1478–1492.
- (20) Agrawal, A. G.; Soman, R. R. *Mini-Rev. Med. Chem.* **2009**, *9*, 638–652.
- (21) Rao, S.; et al. *J. Clin. Oncol.* **2004**, *22*, 3950–3957.
- (22) Van Cutsem, E.; et al. *J. Clin. Oncol.* **2004**, *22*, 1430–1438.
- (23) Zhang, F. L.; et al. *J. Biol. Chem.* **1997**, *272*, 10232–10239.
- (24) Whyte, D. B.; Kirschmeier, P.; Hockenberry, T. N.; Nunez-Oliva, I.; James, L.; Catino, J. J.; Bishop, W. R.; Pai, J.-K. *J. Biol. Chem.* **1997**, *272*, 14459–14464.
- (25) Rowell, C. A.; Kowalczyk, J. J.; Lewis, M. D.; Garcia, A. M. *J. Biol. Chem.* **1997**, *272*, 14093–14097.
- (26) Sparano, J. A.; et al. *J. Clin. Oncol.* **2006**, *24*, 3018.
- (27) Head, J.; Johnston, S. R. D. *Breast Cancer Res.* **2004**, *6*, 262–268.
- (28) Kaklamani, V.; O'Regan, R. M. *Semin. Oncol.* **2004**, *31*, 20–25.
- (29) O'Regan, R. M.; Khuri, F. R. *Endocr. Relat. Cancer* **2004**, *11*, 191–205.
- (30) Kelland, L. R. *Expert Opin. Invest. Drugs* **2003**, *12*, 413–421.
- (31) Johnston, S. R. D.; Kelland, L. R. *Endocr. Relat. Cancer* **2001**, *8*, 227–235.
- (32) Kurzrock, R.; et al. *Blood* **2003**, *102*, 4527–4534.
- (33) Kurzrock, R.; et al. *J. Clin. Oncol.* **2004**, *22*, 1287–1292.
- (34) Alsina, M.; et al. *Blood* **2004**, *103*, 3271–3277.
- (35) Jabbour, E.; Kantarjian, H.; Cortes, J. *Leuk. Lymphoma* **2004**, *45*, 2187–2195.
- (36) Buresh, A.; Perentesis, J.; Rimsza, L.; Kurtin, S.; Heaton, R.; Sugrue, M.; List, A. *Leukemia* **2005**, *19*, 308–310.
- (37) Cortes, J.; et al. *Blood* **2003**, *101*, 1692–1697.
- (38) Zujewski, J.; et al. *J. Clin. Oncol.* **2000**, *18*, 927–941.
- (39) Wang, D. A.; Sefti, S. M. *J. Biol. Chem.* **2005**, *280*, 19243–19249.
- (40) Liu, A. X.; Du, W.; Liu, J. P.; Jessell, T. M.; Prendergast, G. C. *Mol. Cell. Biol.* **2000**, *20*, 6105–6113.
- (41) Kamasani, U.; Huang, M. Z.; DuHadaway, J. B.; Prochownik, E. V.; Donover, P. S.; Prendergast, G. C. *Cancer Res.* **2004**, *64*, 8389–8396.
- (42) Lebowitz, P. F.; Davide, J. P.; Prendergast, G. C. *Mol. Cell. Biol.* **1995**, *15*, 6613–6622.
- (43) Ashar, H. R.; James, L.; Gray, K.; Carr, D.; Black, S.; Armstrong, L.; Bishop, W. R.; Kirschmeier, P. *J. Biol. Chem.* **2000**, *275*, 30451–30457.

- (44) Crespo, N. C.; Ohkanda, J.; Yen, T. J.; Hamilton, A. D.; Sebti, S. M. *J. Biol. Chem.* **2001**, *276*, 16161–16167.
- (45) Hussein, D.; Taylor, S. S. *J. Cell. Sci.* **2002**, *115*, 3403–3414.
- (46) Wang, J.; Kirby, C. E.; Herbst, R. *J. Biol. Chem.* **2002**, *277*, 46659–46668.
- (47) Cates, C. A.; Michael, R. L.; Stayrook, K. R.; Harvey, K. A.; Burke, Y. D.; Randall, S. K.; Crowell, P. L.; Crowell, D. N. *Cancer Lett.* **1996**, *110*, 49–55.
- (48) Basso, A. D.; Mirza, A.; Liu, G. J.; Long, B. J.; Bishop, W. R.; Kirschmeier, P. *J. Biol. Chem.* **2005**, *280*, 31101–31108.
- (49) Barton, R. M.; Worman, H. J. *J. Biol. Chem.* **1999**, *274*, 30008–30018.
- (50) Chakrabarti, D.; Da Silva, T.; Barger, J.; Paquette, S.; Patel, H.; Patterson, S.; Allen, C. M. *J. Biol. Chem.* **2002**, *277*, 42066–42073.
- (51) Wiesner, J.; et al. *Angew. Chem., Int. Ed.* **2004**, *43*, 251–254.
- (52) Glenn, M. P.; et al. *Angew. Chem., Int. Ed.* **2005**, *44*, 4903–4906.
- (53) Nallan, L.; Bauer, K. D.; Bendale, P.; Rivas, K.; Yokoyama, K.; Hornéy, C. P.; Rao Pendyala, P.; Floyd, D.; Lombardo, L. J.; Williams, D. K.; Hamilton, A.; Sebti, S.; Windsor, W. T.; Weber, P. C.; Buckner, F. S.; Chakrabarti, D.; Gelb, M. H.; Van Voorhis, W. C. *J. Med. Chem.* **2005**, *48*, 3704–3713.
- (54) Fletcher, S.; Cummings, C. G.; Rivas, K.; Katt, W. P.; Horney, C.; Buckner, F. S.; Chakrabarti, D.; Sebti, S. M.; Gelb, M. H.; Van Voorhis, W. C.; Hamilton, A. D. *J. Med. Chem.* **2008**, *51*, S176–S197.
- (55) Kohring, K.; et al. *ChemMedChem* **2008**, *3*, 1217–1231.
- (56) Yokoyama, K.; Trobridge, P.; Buckner, F. S.; Van Voorhis, W. C.; Stuart, K. D.; Gelb, M. H. *J. Biol. Chem.* **1998**, *273*, 26497–26505.
- (57) Buckner, F. S.; et al. *J. Biol. Chem.* **2000**, *275*, 21870–21876.
- (58) Panethymitaki, C.; Bowyer, P. W.; Price, H. P.; Leatherbarrow, R. J.; Brown, K. A.; Smith, D. F. *Biochem. J.* **2006**, *396*, 277–285.
- (59) Young, S. G.; Meta, M.; Yang, S. H.; Fong, L. G. *J. Biol. Chem.* **2006**, *281*, 39741–39745.
- (60) Yang, S. H.; et al. *J. Clin. Invest.* **2006**, *116*, 2115–2121.
- (61) Fong, L. G.; Frost, D.; Meta, M.; Qiao, X.; Yang, S. H.; Coffinier, C.; Young, S. G. *Science* **2006**, *311*, 1621–1623.
- (62) Glynn, M. W.; Glover, T. W. *Hum. Mol. Genet.* **2005**, *14*, 2959–2969.
- (63) Chen, W. J.; Andres, D. A.; Goldstein, J. L.; Russell, D. W.; Brown, M. S. *Cell* **1991**, *66*, 327–334.
- (64) Chen, W. J.; Andres, D. A.; Goldstein, J. L.; Brown, M. S. *Proc. Natl. Acad. Sci. U.S.A.* **1991**, *88*, 11368–11372.
- (65) Moores, S. L.; Schaber, M. D.; Mosser, S. D.; Rands, E.; O’Hara, M. B.; Garsky, V. M.; Marshall, M. S.; Pompliano, D. L.; Gibbs, J. B. *J. Biol. Chem.* **1991**, *266*, 14603–14610.
- (66) Reiss, Y.; Goldstein, J. L.; Seabra, M. C.; Casey, P. J.; Brown, M. S. *Cell* **1990**, *62*, 81–88.
- (67) Reiss, Y.; Seabra, M. C.; Armstrong, S. A.; Slaughter, C. A.; Goldstein, J. L.; Brown, M. S. *J. Biol. Chem.* **1991**, *266*, 10672–10677.
- (68) Schafer, W. R.; Rine, J. *Annu. Rev. Genet.* **1992**, *26*, 209–237.
- (69) Glomset, J. A.; Farnsworth, C. C. *Annu. Rev. Cell. Biol.* **1994**, *10*, 181–205.
- (70) Zhang, F. L.; Casey, P. J. *Annu. Rev. Biochem.* **1996**, *65*, 241–269.
- (71) Park, H. W.; Boduluri, S. R.; Moomaw, J. F.; Casey, P. J.; Beese, L. S. *Science* **1997**, *275*, 1800–1804.
- (72) Dolence, J. M.; Rozema, D. B.; Poulter, C. D. *Biochemistry* **1997**, *36*, 9246–9252.
- (73) Kral, A. M.; Diehl, R. E.; deSolms, S. J.; Williams, T. M.; Kohl, N. E.; Omer, C. A. *J. Biol. Chem.* **1997**, *272*, 27319–27323.
- (74) Trueblood, C. E.; Boyartchuk, V. L.; Rine, J. *Proc. Natl. Acad. Sci. U.S.A.* **1997**, *94*, 10774–10779.
- (75) Fu, H. W.; Beese, L. S.; Casey, P. J. *Biochemistry* **1998**, *37*, 4465–4472.
- (76) Wu, Z.; Demma, M.; Strickland, C. L.; Radisky, E. S.; Poulter, C. D.; Le, H. V.; Windsor, W. T. *Biochemistry* **1999**, *38*, 11239–11249.
- (77) Pickett, J. S.; Bowers, K. E.; Hartman, H. L.; Fu, H. W.; Embry, A. C.; Casey, P. J.; Fierke, C. A. *Biochemistry* **2003**, *42*, 9741–9748.
- (78) Pickett, J. S.; Bowers, K. E.; Fierke, C. A. *J. Biol. Chem.* **2003**, *278*, 51243–51250.
- (79) Tobin, D. A.; Pickett, J. S.; Hartman, H. L.; Fierke, C. A.; Penner-Hahn, J. E. *J. Am. Chem. Soc.* **2003**, *125*, 9962–9969.
- (80) Pais, J. E.; Bowers, K. E.; Fierke, C. A. *J. Am. Chem. Soc.* **2006**, *128*, 15086–15087.
- (81) Huang, C. C.; Hightower, K. E.; Fierke, C. A. *Biochemistry* **2000**, *39*, 2593–2602.
- (82) Sousa, S. F.; Fernandes, P. A.; Ramos, M. J. *J. Biol. Inorg. Chem.* **2005**, *10*, 3–10.
- (83) Sousa, S. F.; Fernandes, P. A.; Ramos, M. J. *Biophys. J.* **2005**, *88*, 483–494.
- (84) Sousa, S. F.; Fernandes, P. A.; Ramos, M. J. *J. Mol. Struct. (Theochem)* **2005**, *729*, 125–129.
- (85) Sousa, S. F.; Fernandes, P. A.; Ramos, M. J. *Proteins* **2007**, *66*, 205–218.
- (86) Sousa, S. F.; Fernandes, P. A.; Ramos, M. J. *J. Comput. Chem.* **2007**, *28*, 1160–1168.
- (87) Sousa, S. F.; Fernandes, P. A.; Ramos, M. J. *J. Am. Chem. Soc.* **2007**, *129*, 1378–1385.
- (88) Lenevich, S.; Xu, J. H.; Hosokawa, A.; Cramer, C. J.; Distefano, M. D. *J. Am. Chem. Soc.* **2007**, *129*, 5796–+.
- (89) Cui, G. L.; Wang, B.; Merz, K. M. *Biochemistry* **2005**, *44*, 16513–16523.
- (90) Cui, G.; Merz, K. M. *Biochemistry* **2007**, *46*, 12375–12381.
- (91) Sousa, S. F.; Fernandes, P. A.; Ramos, M. J. *Chemistry* **2009**, *15*, 4243–4247.
- (92) Ho, M. H.; De Vivo, M.; Dal Peraro, M.; Klein, M. L. *J. Chem. Theor. Comput.* **2009**, *5*, 1657–1666.
- (93) Sousa, S. F.; Fernandes, P. A.; Ramos, M. J. *Theor. Chem. Acc.* **2007**, *117*, 171–181.
- (94) Clackson, T.; Wells, J. A. *Science* **1995**, *267*, 383–386.
- (95) Pons, J.; Rajpal, A.; Kirsch, J. F. *Protein Sci.* **1999**, *8*, 958–968.
- (96) Keskin, O.; Ma, B. Y.; Nussinov, R. *J. Mol. Biol.* **2005**, *345*, 1281–1294.
- (97) Bogan, A. A.; Thorn, K. S. *J. Mol. Biol.* **1998**, *280*, 1–9.
- (98) Moreira, I. S.; Fernandes, P. A.; Ramos, M. J. *Proteins* **2007**, *68*, 803–812.
- (99) Lopez, M. A.; Kollman, P. A. *Protein Sci.* **1993**, *2*, 1975–1986.
- (100) Kortemme, T.; Baker, D. *Proc. Natl. Acad. Sci. U.S.A.* **2002**, *99*, 14116–14121.
- (101) Schapira, M.; Totrov, M.; Abagyan, R. *J. Mol. Recognit.* **1999**, *12*, 177–190.
- (102) Aqvist, J.; Medina, C.; Samuelsson, J. E. *Protein Eng.* **1994**, *7*, 385–391.
- (103) Verkhivker, G. M.; Bouzida, D.; Gehlhaar, D. K.; Rejto, P. A.; Freer, S. T.; Rose, P. W. *Proteins* **2002**, *48*, 539–557.
- (104) Massova, I.; Kollman, P. A. *J. Am. Chem. Soc.* **1999**, *121*, 8133–8143.
- (105) Zoete, V.; Meuwly, M. *J. Comput. Chem.* **2006**, *27*, 1843–1857.
- (106) Zoete, V.; Meuwly, M.; Karplus, M. *Proteins* **2005**, *61*, 79–93.
- (107) Moreira, I. S.; Fernandes, P. A.; Ramos, M. J. *J. Comput. Chem.* **2007**, *28*, 644–654.
- (108) Moreira, I. S.; Fernandes, P. A.; Ramos, M. J. *J. Phys. Chem. B* **2006**, *110*, 10962–10969.
- (109) Moreira, I. S.; Fernandes, P. A.; Ramos, M. J. *Int. J. Quantum Chem.* **2007**, *107*, 299–310.
- (110) Moreira, I. S.; Fernandes, P. A.; Ramos, M. J. *Theor. Chem. Acc.* **2008**, *120*, 533–542.
- (111) Bernstein, F. C.; Koetzle, T. F.; Williams, G. J. B.; Meyer, E. F.; Brice, M. D.; Rodgers, J. R.; Kennard, O.; Shimanouchi, T.; Tasumi, M. *J. Mol. Biol.* **1977**, *112*, 535–542.
- (112) Case, D. A. et al. University of California: San Francisco, 2006.
- (113) Long, S. B.; Hancock, P. J.; Kral, A. M.; Hellinga, H. W.; Beese, L. S. *Proc. Natl. Acad. Sci. U.S.A.* **2001**, *98*, 12948–12953.
- (114) Long, S. B.; Casey, P. J.; Beese, L. S. *Nature* **2002**, *419*, 645–650.
- (115) Bowers, K. E.; Fierke, C. A. *Biochemistry* **2004**, *43*, 5256–5265.
- (116) Hartman, H. L.; Bowers, K. E.; Fierke, C. A. *J. Biol. Chem.* **2004**, *279*, 30546–30553.

- (117) Hoops, S. C.; Anderson, K. W.; Merz, K. M., Jr. *J. Am. Chem. Soc.* **1991**, *113*, 8262–8270.
- (118) Sousa, S. F.; Fernandes, P. A.; Ramos, M. J. *Bioorg. Med. Chem.* **2009**, *17*, 3369–3378.
- (119) Sousa, S. F.; Fernandes, P. A.; Ramos, M. J. *Int. J. Quantum Chem.* **2008**, *108*, 1939–1950.
- (120) Sousa, S. F.; Fernandes, P. A.; Ramos, M. J. *J. Phys. Chem. B* **2008**, *112*, 8681–8691.
- (121) Cornell, W. D.; Cieplak, P.; Bayly, C. I.; Gould, I. R.; Merz, K. M.; Ferguson, D. M.; Spellmeyer, D. C.; Fox, T.; Caldwell, J. W.; Kollman, P. A. *J. Am. Chem. Soc.* **1995**, *117*, 5179–5197.
- (122) Hawkins, G. D.; Cramer, C. J.; Truhlar, D. G. *J. Phys. Chem.* **1996**, *100*, 19824–19839.
- (123) Hawkins, G. D.; Cramer, C. J.; Truhlar, D. G. *Chem. Phys. Lett.* **1995**, *246*, 122–129.
- (124) Tsui, V.; Case, D. A. *Biopolymers* **2000**, *56*, 275–291.
- (125) Ryckaert, J. P.; Ciccotti, G.; Berendsen, H. C. J. *Comput. Phys.* **1977**, *23*, 327–341.
- (126) Huo, S.; Massova, I.; Kollman, P. A. *J. Comput. Chem.* **2002**, *23*, 15–27.
- (127) Gohlke, H.; Case, D. A. *J. Comput. Chem.* **2004**, *25*, 238–250.
- (128) Srinivasan, J.; Cheatham, T. E., III; Cieplak, P.; Kollman, P.; Case, D. A. *J. Am. Chem. Soc.* **1998**, *120*, 9401–9409.
- (129) Baron, R.; Hunenberger, P. H.; McCammon, J. A. *J. Chem. Theor. Comput.* **2009**, *5*, 3150–3160.
- (130) Kollman, P. A.; Massova, I.; Reyes, C.; Kuhn, B.; Huo, S.; Chong, L.; Lee, M.; Lee, T.; Duan, Y.; Wang, W.; Donini, O.; Cieplak, P.; Srinivasan, J.; Case, D. A.; Cheatham, T. E., III *Acc. Chem. Res.* **2000**, *33*, 889–897.
- (131) Bradshaw, R. T.; Patel, B. H.; Tate, E. W.; Leatherbarrow, R. J.; Gould, I. R. *Protein Eng., Des. Sel.* **2011**, *24*, 197–207.
- (132) Sousa, S. F.; Fernandes, P. A.; Ramos, M. J. *J. Phys. Chem. B* **2011**, *115*, 7045–7057.
- (133) Zoete, V.; Michielin, O. *Proteins* **2007**, *67*, 1026–1047.
- (134) Massova, I.; Kollman, P. A. *Perspect. Drug Discovery Des.* **2000**, *18*, 113–135.
- (135) Humphrey, W.; Dalke, A.; Schulten, K. *J. Mol. Graphics Modell.* **1996**, *14*, 33–&.
- (136) Laskowski, R. A.; Hutchinson, E. G.; Michie, A. D.; Wallace, A. C.; Jones, M. L.; Thornton, J. M. *Trends Biochem. Sci.* **1997**, *22*, 488–490.
- (137) Laskowski, R. A. *Nucl. Acid Res.* **2001**, *29*, 221–222.
- (138) Glaser, F.; Rosenberg, Y.; Kessel, A.; Pupko, T.; Ben-Tal, N. *Proteins* **2005**, *58*, 610–617.
- (139) Pupko, T.; Bekk, R. E.; Mayrose, I.; Glaser, F.; Ben-Tal, N. *Bioinformatics* **2002**, *18*, S71–S77.
- (140) Dodge, C.; Schneider, R.; Sander, C. *Nucleic Acids Res.* **1998**, *26*, 313–315.
- (141) Sander, C.; Schneider, R. *Proteins* **1991**, *9*, 56–68.
- (142) Long, S. B.; Casey, P. J.; Beese, L. S. *Biochemistry* **1998**, *37*, 9612–9618.
- (143) Dunten, P.; Kammlott, U.; Crowther, R.; Weber, D.; Palermo, R.; Birktoft, J. *Biochemistry* **1998**, *37*, 7907–7912.